

## Synthesis Gas Production by Methane Partial Oxidation on Ni/Fe<sub>3</sub>O<sub>4</sub>-Ce<sub>0.75</sub>Zr<sub>0.25</sub>O<sub>2</sub> Catalysts: Kinetic Study

M. I. Sosa Vazquez, J. Salinas Gutierrez, D. Delgado Vigil, V. Collins-Martinez and A. Lopez Ortiz\*

Departamento de Materiales Nanoestructurados, Centro de Investigación en Materiales Avanzados,  
S. C. Miguel de Cervantes 120, Chihuahua, Chih., México 31109.

Received: October 30, 2010, Accepted: January 20, 2011, Available online: April 06, 2011

**Abstract:** Fe<sub>3</sub>O<sub>4</sub>-Ce<sub>0.75</sub>Zr<sub>0.25</sub>O<sub>2</sub> (FeCZ) is an oxygen carrier material aimed to produce syngas through methane partial oxidation in absence of oxygen gas feed. The objective of the present research is to study the catalytic effect of Ni on FeCZ using an evaluation of the global kinetics (activation energy, reaction rate, order and constant) of its reaction with methane for syngas production. FeCZ and 0.05NiFeCZ (Ni/Fe = 0.05 molar ratio) were synthesized through co-precipitation of their precursor nitrate salts, while 2NiFeCZ was prepared by impregnation of FeCZ with a nickel nitrate solution to obtain a 2 %W Ni material. Samples were calcined at 950°C during 4 hours in air. Kinetic study of oxygen carriers (FeCZ, 0.05NiFeCZ and 2NiFeCZ) reduction with methane was followed through thermogravimetric analysis (TGA) at 5, 7.5 and 10% CH<sub>4</sub>/Ar and 600, 650 and 700°C. Initial reaction rate was obtained from the slope of the linear region of the weight change signal as a function of time. Results indicate a first order global reaction rate for all materials. Activation energies for samples FeCZ, 0.05NiFeCZ and 2NiFeCZ were 52.2, 39.5 and 28.3 Kcal/mol, respectively. Thus, reflecting the catalytic effect of Ni over the FeCZ global reaction rate.

**Keywords:** Syngas production, methane partial oxidation, oxygen carrier, kinetic study

### 1. INTRODUCTION

Hydrogen, as an energy carrier, has been considered to be an environmentally acceptable option to face the global warming problem that today harms the planet, because during its use does not involve the production of greenhouse gases (CO<sub>2</sub>). Nowadays, world's demand for hydrogen is high (approximately 70 million metric tons per year) with industrial applications such as: oil refining, metallurgy, food and electronic industries among others [1]. Recently, new hydrogen applications have emerged. Among those are fuel cells, which employ hydrogen and oxygen to produce electric energy at higher efficiencies than actual internal combustion engines.

With equal importance as hydrogen is the mixture of carbon monoxide and hydrogen (CO +H<sub>2</sub>), commonly known as synthesis gas or "syngas", which today is used as a raw material for many industrial applications. Furthermore, this mixture is also used to produce hydrogen through the water gas shift reaction process

(WGS).

The conversion of methane to syngas is a crucial step in the use of natural gas towards the production of hydrogen. Moreover, this syngas mixture is a fundamental raw material for the Fischer Tropsch (FT) process, where is converted to liquid hydrocarbons to produce several synthetic substitutes of petroleum, such as: lube oils, and all kinds of liquid fuels [2]. The use of syngas through the FT process (for the production of liquid fuels) combined with a growing demand of a vast number of chemicals derived from this process, have converted this mixture in an strategic factor for nations with growing economies facing the continuous increase in oil prices during the last decade [3].

To supply this growing demand for syngas and hydrogen there has been a growing interest in the scientific community towards research focused in the reduction of operating costs and increasing efficiencies in the related processes. A strategy that has been identified as potentially effective is the introduction of modifications to the conventional hydrogen production processes from fossil fuels; steam reforming, coal gasification and partial oxidation of hydrocarbons. Some important advantages of this strategy are: to take

\*To whom correspondence should be addressed:

Email: alejandro.lopez@cimav.edu.mx

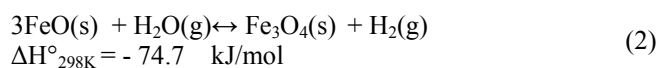
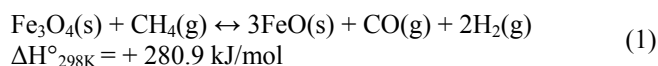
Phone: +52-614-439-4815; Fax: +52-614-439-1130

advantage of the large experience gained through the years in the operation of these processes and the reutilization of the existing infrastructure around the world. Additionally, derived from these modifications, it is possible to significantly reduce CO<sub>2</sub> emissions in these processes, thus decreasing today's global warming effects that harm our planet. As a consequence, the innovations introduced to conventional processes have become an essential bridge to reach the desired hydrogen economy [4].

One modification to the conventional technology for hydrogen production is the partial oxidation of methane by oxygen carriers that consist in two steps. In the first step, the oxygen required for the partial oxidation is supplied by a material that stores oxygen in its structure such as a metal oxide (MeO). This oxygen is released under a reducing atmosphere (methane) producing syngas (CO + H<sub>2</sub>) and the reduced metal (Me). In the second step the reduced material (Me) is re-oxidized with water vapor producing additional hydrogen as a product. Finally, the oxidized material is sent back to the initial step for its reutilization in the process. This material (metal oxide), which is able to release and store oxygen in a cyclic manner has been called an oxygen carrier (OC) [5]. If carbon deposition would not occur over the surface of the solids, theoretically, a high purity hydrogen product could be obtained during reduction and re-oxidation of the material. This last can be accomplished without the use of additional hydrogen purification processes such as WGS and PSA (pressure swing adsorption). However, this carbon deposition issue has not been properly evaluated in many studies reported in the literature [6-11].

There exist a large number of materials that have been reported in the literature as oxygen carriers for different redox applications (partial oxidation, chemical looping, etc.) and are based on oxides of Fe, Ni, Cu, Mn and Co supported on Al<sub>2</sub>O<sub>3</sub>, SiO<sub>2</sub>, TiO<sub>2</sub>, ZrO<sub>2</sub>, NiAl<sub>2</sub>O<sub>4</sub>, MgAl<sub>2</sub>O<sub>4</sub> as well as unsupported [12-22]. However, because iron oxide is an environmentally friendly material, thermodynamically able to be reduced with methane and re-oxidized with water vapor [23] and with high availability and low price, make of this material an ideal selection as the main oxygen carrier to be used for the purpose of the present investigation.

Methane partial oxidation from iron oxide to produce syngas and its re-oxidation with water vapor to produce hydrogen is performed according to the following reactions:



Khun et al., [24] studied the reduction of magnetite (Fe<sub>3</sub>O<sub>4</sub>) with methane towards the production of syngas and metallic iron. Hacker et al., [25, 26] also reported this as the "steam iron process", in which iron oxide was reduced from biomass decomposition gases, while the reduced metal reacted with steam to produce high purity hydrogen. Researchers have concentrated their work in increasing iron oxide reactivity with methane and decreasing the working temperature through the use of promoters such as Cu and Ni [11, 27, 28]. However, they have found sintering problems of these materials due to the high operating temperature. Oxides of Cr, Co and Cu have been reported to alleviate this problem and to prevent the formation of iron carbides and graphite [29]. The addition

of rare earths such as ceria have also been used to promote iron oxide reducibility due to its high oxygen storage capacity (OSC) and ability to easily store and release its lattice oxygen. This promoting effect of ceria (CeO<sub>2</sub>) over iron oxide towards methane oxidation has been reported by Kang and Wang [30] and Bao et al., [31], who demonstrated the positive effect of ceria in the catalytic oxidation of CO. Ceria inclusion have been shown to increase the activity and thermal stability of iron oxide (Fe<sub>3</sub>O<sub>4</sub>) after several (seven) redox cycles as recently reported by Lorente et al., [32]. It has been recognized that the presence of CeO<sub>2</sub> as promoter, participates in the removal of the adsorbed carbon over the surface of the oxygen carrier during the methane oxidation with Fe<sub>3</sub>O<sub>4</sub> lattice oxygen [33]. It has been reported that the inclusion of ceria within zirconium oxide (ZrO<sub>2</sub>) enhances this promotion [5, 34, 35] and increases its catalytic activity by limiting the superficial carbon deposition in greater amount than the individual use of ceria. Additionally, ZrO<sub>2</sub> have been able to keep Fe<sub>3</sub>O<sub>4</sub> stability at temperatures as high as 1600°C as reported by Kodama et al., [36] and Gokon et al., [37] in their cyclic experiments aiming the Fe<sub>3</sub>O<sub>4</sub> (supported in ZrO<sub>2</sub>) thermochemical decomposition for hydrogen production.

The combination of CeO<sub>2</sub>, which is recognized by its ability to cyclically store and release oxygen within its structure (transfer oxygen atoms) and ZrO<sub>2</sub>, that enhances ceria OSC [38] produces a solid solution material (Ce<sub>0.75</sub>Zr<sub>0.25</sub>O<sub>2</sub>, CZ). This novel material was developed for three-way catalyst applications in the automotive industry [30].

Nevertheless, CZ unique features towards the partial oxidation of methane above described, its oxygen storage capacity (OSC) is significantly limited. Recently Sosa et al., [5] used the high OSC of Fe<sub>3</sub>O<sub>4</sub> and the ability of CZ to store and release oxygen to produce a material with a high OSC and being able to partially oxidize methane to produce hydrogen. They found that the presence of CZ (Ce<sub>0.75</sub>Zr<sub>0.25</sub>O<sub>2</sub>) generates an increase in Fe<sub>3</sub>O<sub>4</sub> reducibility accompanied with a decrease in its reduction temperature in hydrogen as well as in methane atmospheres.

Furthermore, Ni has been recognized by its catalytic action towards methane partial oxidation in CeO<sub>2</sub> and in ZrO<sub>2</sub> supports. With ceria, the effect is reflected in higher methane conversions, while zirconia allows the elimination of the adsorbed carbon over the catalyst surface, thus promoting CO formation [39]. Ni surface specifically, has been reported to catalyze the methane decomposition and to present a selective action towards syngas formation [40, 41 42]. Finally, in experiments in this laboratory the addition of CZ to Fe<sub>3</sub>O<sub>4</sub> (Fe) produced an increase in methane oxidation conversion at 700°C of twice with respect to Fe<sub>3</sub>O<sub>4</sub> and this was associated to a catalytic effect of Ni in FeCZ (Fe<sub>3</sub>O<sub>4</sub>-Ce<sub>0.75</sub>Zr<sub>0.25</sub>O<sub>2</sub>) [5]. Even though FeCZ reported values in the literature show a catalytic effect of Ni towards an increase in methane conversion, an appropriate kinetic study is needed in order to properly evaluate such effect.

Therefore, the objective of the present research is the evaluation of the global kinetic parameters (reaction rate, constant, order and activation energy) of FeCZ during its reduction with methane and to assess the Ni catalytic effect on the oxygen carrier (FeCZ). The kinetic study of this material is a crucial step to realistically determine the feasibility of a potential process and to provide a better understanding of the influence of reaction conditions over the ma-

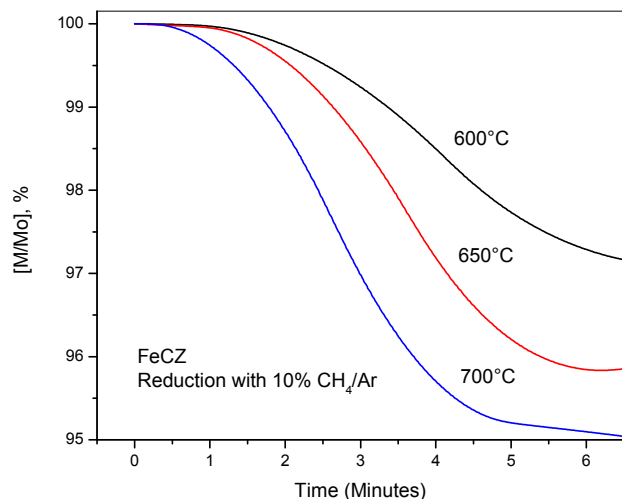


Figure 1. Temperature effect of sample FeCZ at 10% CH<sub>4</sub>/Ar

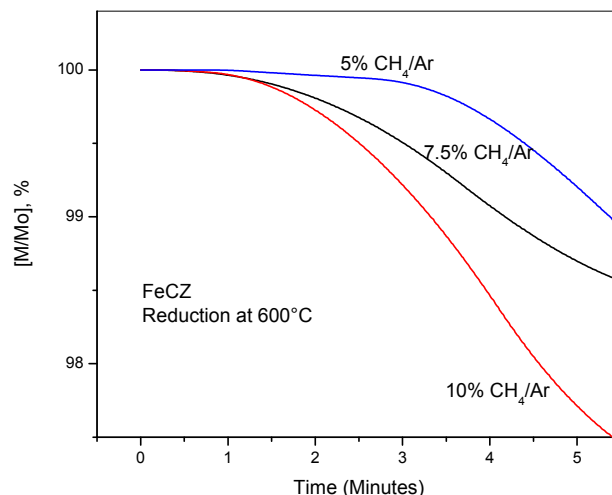


Figure 2. CH<sub>4</sub> concentration effect for sample FeCZ at 600°C

terial and to help postulate in the future a possible reaction mechanism that fits the kinetic results of the process. It is important to notice that results of the present kinetic study must be considered as a first attempt to describe the reaction rate of the hydrogen and/or syngas production step of the process and this can be used (with the appropriate considerations) to predict the process performance under several operating conditions in future studies.

## 2. EXPERIMENTAL

FeCZ (Fe<sub>3</sub>O<sub>4</sub>-Ce<sub>0.75</sub>Zr<sub>0.25</sub>O<sub>2</sub>) and 0.05NiFeCZ (0.05 mols of Ni per mol of Fe) synthesis was performed by co-precipitation of Fe(NO<sub>3</sub>)<sub>3</sub>·9H<sub>2</sub>O (J.T. Baker), (NH<sub>4</sub>)<sub>2</sub>Ce(NO<sub>3</sub>)<sub>6</sub> (Merck) and ZrOCl·8H<sub>2</sub>O (spectrum Chemical Mfg-Corp) and Ni(NO<sub>3</sub>) (J. T. Baker). Each one of these reagents was dissolved in 50 ml of de-ionized water and later was precipitated with an ammonium hydroxide stoichiometric solution. The addition of the precipitant solution was performed using a peristaltic pump at a rate of 3 ml/min followed by heating at 60°C to dryness. The sample was then calcined at 900°C by 4 hours. The addition of Ni to FeCZ (in the case of sample 2NiFeCZ) was made by incipient impregnation employing a nickel nitrate solution in order to obtain a sample with 2%W Ni and this was called 2NiFeCZ. The amount of 2%W was carefully calculated in order to insure that amount of Ni used in both syntheses (precipitation and impregnation) were the same. Finally, the sample was dried at 100°C and later calcined at 900°C during 4 hours.

Follow up of oxygen carriers (FeCZ, 0.05NiFeCZ and 2NiFeCZ)

reductions was performed by thermogravimetric analysis (TGA) in a Q500 from TA-Instruments under a 100 ml/min flowrate and at different methane concentrations and temperatures. Table 1 shows a matrix of the tests made for the present kinetic study, where mixtures of 5, 7.5 and 10% CH<sub>4</sub> at temperatures of 600, 650 and 700°C were employed.

TGA experimental procedure is described as follows: 20 mg of sample was placed in a platinum-made sample holder and then heated up to the desired reaction temperature under an Argon atmosphere. Once the reaction temperature was reached the selected CH<sub>4</sub>/Ar gas mixture was introduced. The reaction started and the follow up was made by the weight change (%W) signal with respect to time.

## 3. RESULTS AND DISCUSSION

### 3.1. Temperature Effect

Figure 1 presents the TGA response in %W vs time (minutes) for sample FeCZ at a 10% CH<sub>4</sub>/Ar concentration and 600, 650 and 700°C. Tests presented in this Figure were selected for illustrative purposes. In this Figure, a strong temperature effect is evident over the initial reaction rate. The separation between curves indicates a high dependence of the initial reaction rate with respect to temperature.

### 3.2. Feed Gas Composition

Figure 2 shows the TGA response in %W vs time for sample FeCZ at 600°C and feed concentrations of 5, 7.5 and 10% CH<sub>4</sub>/Ar.

Table 1. TGA matrix test for the global kinetic study

| Material   | Temperature            |                          |                         |                        |                          |                         |                        |                          |                         |
|------------|------------------------|--------------------------|-------------------------|------------------------|--------------------------|-------------------------|------------------------|--------------------------|-------------------------|
|            | 600°C                  |                          |                         | 650°C                  |                          |                         | 700°C                  |                          |                         |
| FeCZ       | 5% CH <sub>4</sub> /Ar | 7.5% CH <sub>4</sub> /Ar | 10% CH <sub>4</sub> /Ar | 5% CH <sub>4</sub> /Ar | 7.5% CH <sub>4</sub> /Ar | 10% CH <sub>4</sub> /Ar | 5% CH <sub>4</sub> /Ar | 7.5% CH <sub>4</sub> /Ar | 10% CH <sub>4</sub> /Ar |
| 0.05NiFeCZ | 5% CH <sub>4</sub> /Ar | 7.5% CH <sub>4</sub> /Ar | 10% CH <sub>4</sub> /Ar | 5% CH <sub>4</sub> /Ar | 7.5% CH <sub>4</sub> /Ar | 10% CH <sub>4</sub> /Ar | 5% CH <sub>4</sub> /Ar | 7.5% CH <sub>4</sub> /Ar | 10% CH <sub>4</sub> /Ar |
| 2NiFeCZ    | 5% CH <sub>4</sub> /Ar | 7.5% CH <sub>4</sub> /Ar | 10% CH <sub>4</sub> /Ar | 5% CH <sub>4</sub> /Ar | 7.5% CH <sub>4</sub> /Ar | 10% CH <sub>4</sub> /Ar | 5% CH <sub>4</sub> /Ar | 7.5% CH <sub>4</sub> /Ar | 10% CH <sub>4</sub> /Ar |

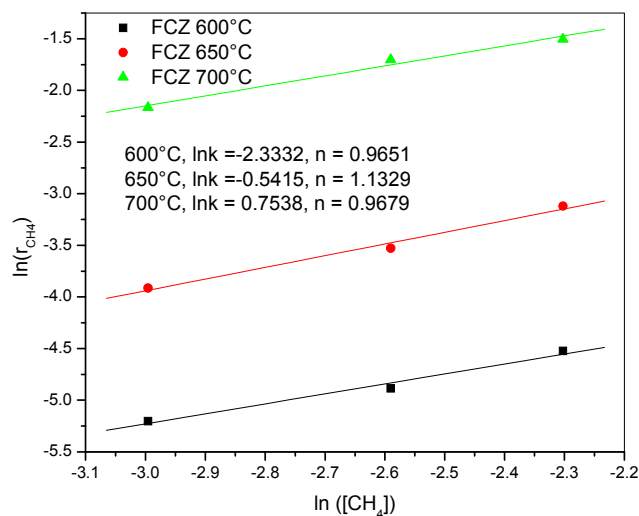


Figure 3. Reaction order calculation plot for sample FeCZ

In this Figure it can be observed a strong methane concentration effect over the initial reaction rate. Especially in concentrations between 5 and 7.5% CH<sub>4</sub>, because the separation of these test curves is significant, while separation between 7.5 and 10% CH<sub>4</sub> is somewhat small. These results suggest that at small CH<sub>4</sub> concentrations (5%) diffusional effects of this gas at the interior of the reacting particles are more accentuated than at higher concentrations (7.5 and 10% CH<sub>4</sub>). Since, according to results recently published by Sosa et al., [5] the two materials 0.05NiFeCZ and 2NiFeCZ presented 5.3 and 1.8 m<sup>2</sup>/g BET surface areas, respectively and practically no porosity. However, a deeper analysis of the global kinetics and initial reaction rate is needed in order to properly evaluate this reaction system.

### 3.3. Global Reaction Rate

In a TGA thermogram (like the one shown in Figure 2) the initial reaction rate can be reasonable estimated, assuming that this is proportional to the slope of the signal curve (%W vs time) within the initial linear region. The initial reaction rates were evaluated for

Table 2. Initial reaction rate of oxygen carriers with CH<sub>4</sub>

| Material   | [CH <sub>4</sub> ], % | Initial Reaction Rate, $r_A$ [min <sup>-1</sup> ] |         |         |
|------------|-----------------------|---|---------|---------|
|            |                       | 600°C   | 650°C   | 700°C   |
| FeCZ       | 5.0                   | 0.00550   | 0.01997 | 0.11459 |
|            | 7.5                   | 0.00755   | 0.02932 | 0.18211 |
|            | 10.0                  | 0.01084   | 0.04419 | 0.22223 |
| 0.05NiFeCZ | 5.0                   | 0.01332   | 0.02736 | 0.16959 |
|            | 7.5                   | 0.01857   | 0.03969 | 0.25131 |
|            | 10.0                  | 0.02673   | 0.05994 | 0.32223 |
| 2NiFeCZ    | 5.0                   | 0.01132   | 0.03019 | 0.17532 |
|            | 7.5                   | 0.01636   | 0.04379 | 0.25860 |
|            | 10.0                  | 0.02256   | 0.05851 | 0.30890 |

each one of the 27 tests that were performed. Three materials; FeCZ, 0.05NiFeCZ and 2NiFeCZ, three temperatures; 600, 650 and 700°C and three concentrations; 5, 7.5 and 10% CH<sub>4</sub>/Ar and results are presented in Table 2.

According to the general reaction rate equation this initial rate is equal to the following expression:

$$r_A = k C_A^n \quad (3)$$

where k is the reaction rate constant, C<sub>A</sub> is the CH<sub>4</sub> concentration in molar fraction and n is the reaction order with respect to C<sub>A</sub>.

### 3.4. Reaction Order

Figure 3 presents the calculation of the reaction order for the FeCZ oxygen carrier with respect to methane concentration evaluated under reaction conditions previously described in the experimental section. In this Figure the logarithm of the reaction rate vs the logarithm of the methane concentration is plotted. Results of the linear regression analysis at each temperature lead to a linear equation, where the y axis intercept represents the logarithm of the reaction rate constant (k) and the slope (n) the reaction order at a specific temperature.

According to Figure 3 reaction order for the FeCZ oxygen carrier varies between 0.96 and 1. Therefore, it can be concluded that this sample presents a first reaction order with respect to methane concentration.

Literature related to Fe<sub>3</sub>O<sub>4</sub> reduction is focused in the reaction of this oxygen carrier with hydrogen and in some cases with H<sub>2</sub>/CO reducing mixtures [43, 44 45]. Although there exist a great deal of discrepancy among the proposed models, there is agreement, among literature studies, in the fact that Fe<sub>3</sub>O<sub>4</sub> reduction with hydrogen presents first order kinetics. This fact is important to keep it in mind, since during the reduction process of Fe<sub>3</sub>O<sub>4</sub> with methane the first step is the reduction of the metal oxide with the hydrogen generated by methane decomposition over the surface of the oxygen carrier. However, there have been few studies related to the Fe<sub>3</sub>O<sub>4</sub> reduction kinetics with hydrocarbons and especially with methane. Among those reported studies of Fe<sub>3</sub>O<sub>4</sub> reduction with methane is the case of Ghosh et al., [46] who determined that during the reduction process there are two main fundamental steps; the first is the decomposition of methane in carbon and hydrogen according to the following reaction:



The second is given by the reduction of Fe<sub>3</sub>O<sub>4</sub> by hydrogen, carbon and carbon monoxide according to the following possible reactions:



where [O] is the lattice oxygen present in Fe<sub>3</sub>O<sub>4</sub>.

Furthermore, it was reported that reduction kinetics of methane with respect to the reduction with hydrogen is about 4 ½ times slower [43, 46] at high temperatures (≈ 930°C). As mentioned before, in the literature is reported that the reduction kinetics of Fe<sub>3</sub>O<sub>4</sub> with hydrogen is of first order. Therefore, it can be presumed that

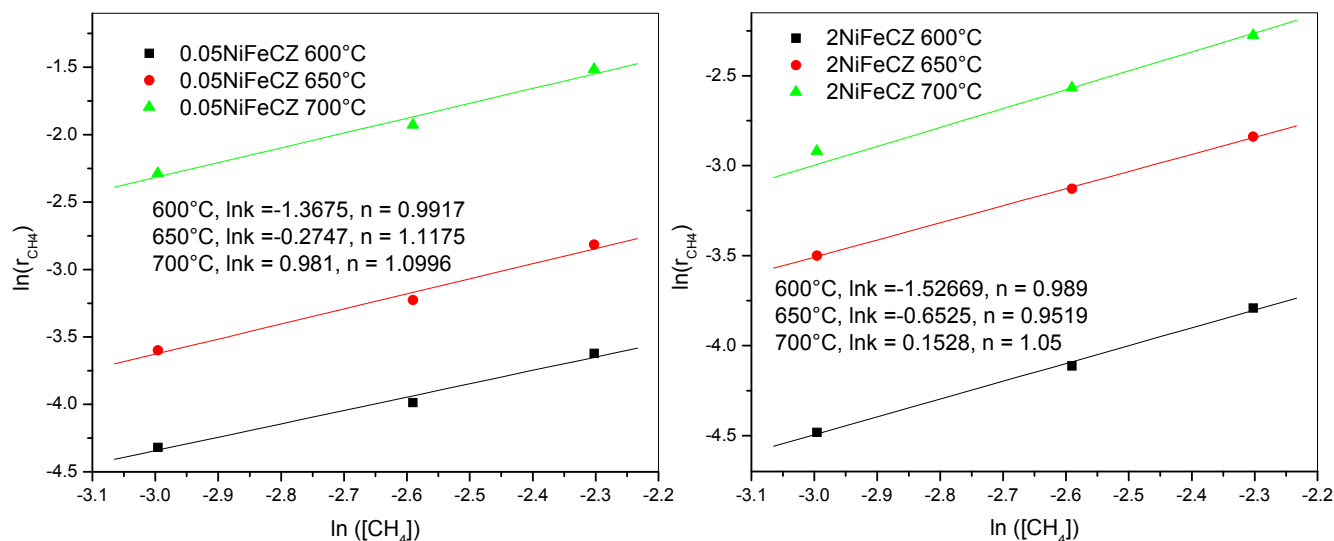


Figure 4. Reaction order calculation plots for samples 0.05NiFeCZ and 2NiFeCZ

for the case of sample FeCZ, the general reaction scheme implies the decomposition of methane into carbon and hydrogen with the consequent reduction of the metal oxide from the generated hydrogen and the subsequent production of carbon oxides (CO and CO<sub>2</sub>) coming from the lattice oxygen, which is provided by Fe<sub>3</sub>O<sub>4</sub>. This phenomenon is further promoted by the presence of CZ due to its high oxygen mobility. These results agree well with data from the initial reduction reaction for sample FeCZ with methane obtained in this laboratory and recently reported [5].

Figure 4 shows the calculation of the reaction order for samples 0.05NiFeCZ and 2NiFeCZ, which were promoted with Ni as catalyst. For both samples, the reaction order varied between 0.98 and 1 with a good linear correlation. Therefore, here also it can be considered that the global reaction order is approximately of one with respect to methane concentration. It is important to notice that the reaction order for samples with Ni is closer to unity than with sample FeCZ.

In the literature it is reported that Ni presents a catalytic activity towards methane partial oxidation, in CeO<sub>2</sub> as well as in ZrO<sub>2</sub> as supports. Its effect is reflected in an increase of methane conversion and in the elimination of the adsorbed carbon over the surface, thus promoting CO formation [39]. The Ni surface specifically as catalyst has been reported to promote methane decomposition and to present a selective action towards the formation of syngas [40, 41, 42]. Therefore, it can be expected of Ni to increase the reaction rate due to its catalytic effect, as can be seen in results of Table 2, where the addition of Ni to FeCZ at 600°C (samples 0.05NiFeCZ and 2NiFeCZ) produce and increase from 1.3 to 2.5 times in its initial reaction rate.

### 3.5. Activation Energy

Once determined the values of the reaction rate constants ( $k$ ) and reaction order ( $n$ ) the next step is the calculation of the activation energy by means of the Arrhenius equation:

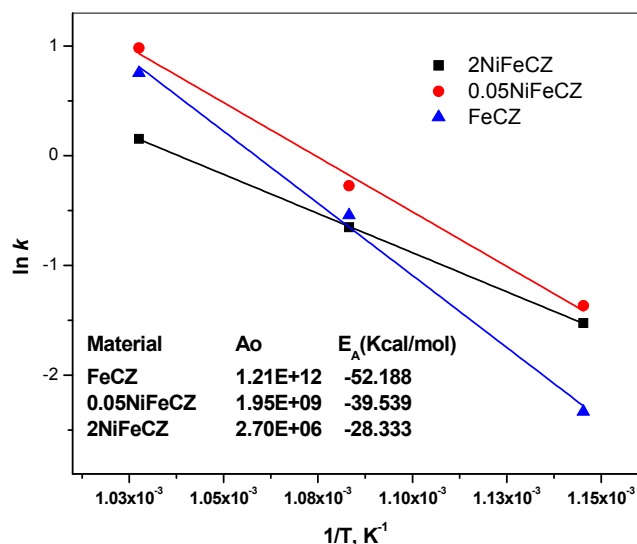


Figure 5. Activation energies for the oxygen carriers studied

$$k = A_o e^{\frac{E_A}{RT}} \quad (8)$$

Figure 5 presents the Arrhenius plot ( $\ln k$  vs  $1/T$ ) for the three oxygen carriers studied in the present research (FeCZ, 0.05NiFeCZ and 2NiFeCZ).

In this Figure it can be observed that sample FeCZ presents the greatest activation energy among all oxygen carriers with a value of 52.18 Kcal/mol. It is useful to compare this last value with reported activation energies reported in the literature for similar metal oxides. For example, NiO reduction with methane presents an  $E_A = 63.9$  Kcal/mol in a temperature range of 750-1000°C, while for ZnO this value was found to be  $E_A = 67.09$  Kcal/mol in a tempera-

ture range of 875-930°C [48]. Whereas, for Fe<sub>3</sub>O<sub>4</sub> its reduction with methane presents a value of 52.7 Kcal/mol in a temperature range of 875-950°C [46], which is a very close value to the one found for FeCZ in the present research. This FeCZ activation energy value is greater to the characteristic apparent activation energy of a surface chemically controlled reaction ( $E_A = 18-20$  Kcal/mol) [49]. Therefore, it can be assumed that FeCZ reduction kinetics is also controlled by this phenomenon. It is important to mention that when methane is the reducing agent at high temperatures, this tends to generate carbon deposits over the surface of the oxygen carrier, which may eventually block surface pores in the material causing a substantial reaction kinetics reduction. This can be observed towards the middle of the reaction as pointed out by recent results reported by Sosa et al., [5]. This behavior has been reported to be severe at higher temperatures than 900°C [47]. However, the present study is focused on temperatures below 700°C, where this carbon deposition problem is expected to be no that significant.

Results of Figure 5 allows to observe that the presence of Ni as catalyst has a positive effect over the global reaction rate, since it leads to a reduction of around 25% and 50% for samples 0.05NiFeCZ and 2NiFeCZ, respectively with respect to the apparent activation energy of FeCZ. Finally, according to the above obtained results, the global kinetic expressions for each one of the oxygen carriers are as follows:

$$-r_A[\text{FeCZ}] = 1.21E + 12 \exp(-52.188 / RT) y_{CH_4} \quad (9)$$

$$-r_A[0.05\text{NiFeCZ}] = 1.95E + 09 \exp(-39.539 / RT) y_{CH_4} \quad (10)$$

$$-r_A[2\text{NiFeCZ}] = 2.70E + 06 \exp(-28.333 / RT) y_{CH_4} \quad (11)$$

#### 4. CONCLUSIONS

The initial reaction rate was obtained by calculating the slope within the linear region of the weight change versus time TGA signal for each oxygen carrier (FeCZ, 0.05NiFeCZ and 2NiFeCZ). A strong temperature and methane concentration effects over the initial reaction rate were found for all studied materials. Results indicated a global first reaction order for all the oxygen carriers in the temperature and methane concentration ranges studied. Activation energies for samples FeCZ, 0.05NiFeCZ and 2NiFeCZ were 52.2, 39.5, and 28.3 Kcal/mol, respectively, which reflect the catalytic influence of Ni over the global reaction rate of FeCZ. These apparent activation energy values indicate that the reaction is presumably controlled by the surface chemical reaction.

#### 5. ACKNOWLEDGEMENTS

The authors gratefully acknowledge to CONACYT for funding of this research under the grant SEP-CONACYT No. 403596. Also, the help of Eng. Enrique Torres and M. Sc. Daniel Lardizabal is acknowledged by their valuable support during the experimental activities of the present research.

#### REFERENCES

[1] World Nuclear Association, Transport and the Hydrogen Economy, Available at <http://www.worldnuclear.org/info/inf70.html>

- , June (2010).
- [2] Proceedings of the 2001 Hydrogen Program Review Meeting, U.S., DOE, Hydrogen Program, (2001).  
[http://www1.eere.energy.gov/hydrogenandfuelcells/annual\\_review\\_2001.html](http://www1.eere.energy.gov/hydrogenandfuelcells/annual_review_2001.html).
- [3] T.S. Christensen, and I.I. Primdahl, *Hydrocarbon Process. Int. Ed.*, 73, 39 (1994).
- [4] A. López Ortiz, T. De los Ríos, J. Salinas Gutiérrez, D. Delgado Vigil, V. Collins-Martínez, *Hidrogeno, Introducción a la energía limpia*, Editorial UACM, 25 (2009).
- [5] M.I. Sosa Vázquez, M.D. Delgado Vigil, J. Salinas Gutiérrez, V. Collins Martínez A. López Ortiz, *J. New Mater Electrochem. Syst.*, 12, 029 (2009).
- [6] R. Sime, J. Kuehni, L. Dsouza, E. Elizondo, S. Biollaz, *Int. J. Hydrogen Energy*, 28, 491 (2003).
- [7] J. Wolf, J. Yan, *Int. J. Energy Res.*, 29, 739 (2005).
- [8] P. Chiesa, G. Lozza, A. Malandrino, M. Romano, V. Piccolo, *Int. J. Hydrogen Energy*, 33, 2233 (2008).
- [9] K. Otsuka, S. Takenaka, *J. Jpn. Petrol Inst.*, 47, 377 (2004).
- [10] K. Otsuka, Y. Wang, E. Sunada, I. Yamanaka, *J. Catal.*, 175, 152 (1998).
- [11] S. Takenaka, T. Kaburagi, C. Yamada, K. Nomura, K. Otsuka, *J. Catal.*, 228, 66 (2004).
- [12] Q. Zafar, T. Mattisson, B. Gevert, *Energy Fuels*, 20, 34 (2006).
- [13] K.E. Sedor, M.M. Hossain, H.I de Lasa, *Chem Eng Sci.*, 63, 11, 2994 (2008).
- [14] M.M. Hossain, K.E. Sedor, de Lasa, H.I. *Chem Eng Sci.*, 62, 5464 (2007).
- [15] T. Mattisson, M. Johansson, M. Lyngfelt, *Energy & Fuel*, 17, 643 (2003).
- [16] T. Mattisson, M. Johansson, M. Lyngfelt, *Energy Fuel*, 18, 628 (2004).
- [17] T. Mattisson, M. Johansson, M. Lyngfelt, *Fuel*, 85, 736 (2006).
- [18] P. Cho, T. Mattisson, M. Lyngfelt, *Ind. Eng. Chem. Res.*, 45, 968 (2006).
- [19] L.F. de Diego, F. Garcia-Labiano, P. Gayan, J. Celaya, J.M. Palacios, J. Adanez, *Fuel*, 86, 1036 (2007).
- [20] A. Abad, T. Mattisson, M. Lyngfelt, A. Ryden, *Fuel*, 85, 1174 (2006).
- [21] A. Abad, J. Adanez, F. Garcia-Labiano, L. de Diego, P. Gayan, J. Celaya, *Chem Eng Sci.*, 62, 533 (2007).
- [22] A. Abad, T. Mattisson, A. Lyngfelt, M. Johansson, *Fuel*, 86, 1021 (2007).
- [23] M. Mohammad, M. Hossain, H.I. de Lasa, *Chem Eng Sci.*, 63, 4433 (2008).
- [24] A. Steinfeld, P. Kuhn, *Energy*, 18, 239 (1993).
- [25] V. Hacker, G. Faleschini, H. Fuchs, R. Fankhauser, G. Simader, M. Ghaemi, B. Spreitz, K. Friedrich, *J Power Sour.*, 71, 226 (1998).
- [26] V. Hacker, R. Fankhauser, G. Faleschini, H. Fuchs, K. Friedrich, M. Muhr, K. Kordesch, *J. Power Sour.*, 86, 531 (2000).
- [27] S. Takenaka, V.T.D. Son, and K. Otsuka, *Energy Fuels*, 18,

- 820 (2004).
- [28]S. Takenaka, K. Nomura, N. Hanaizumi, and K. Otsuka, *Appl Catal A.*, 282, 333 (2005).
- [29]K.S. Kang, C.H. Kim, W.C. Cho, K.K. Bae, S.W. Woo, and C.S. Park, *Int. J. Hydrogen Energy*, 33, 4560 (2008).
- [30]Z. Kang, L. Wang, *Adv. Mater.*, 15, 521 (2003).
- [31]H. Bao, X. Chen, J. Fang, Z. Jiang, and W. Huang, *Catal. Lett.*, 125, 160 (2008).
- [32]E. Lorente, J.A. Peña, J. Herguido, *J Power Sourc.*, 192, 224 (2009).
- [33]E. Aneggi, C. De Leitenburg, G. Dolcetti, A. Trovarelli, *Catal. Today*, 114, 40 (2006).
- [34]D.H. Lee, K.S. Cha, Y.S. Lee, K.S. Kang, C.S. Park, and Y.H. Kim, *Int J Hydrogen Energy*, 34, 1417 (2009).
- [35]V. Galvita, K. Sundmacher, *Appl Catal A.*, 289, 121 (2005).
- [36]T. Kodama, Y. Nakamuro, T. Mizuno, *J. Solar Energy Engineering, of the ASME*, 128, 3 (2006).
- [37]N. Gokon, H. Murayama, J. Umeda, T. Hatamachi, T. Kodama, *Int. J. Hydrogen Energy*, 34, 1208 (2009).
- [38]H. Sobukawa, *R&D Rev. Toyota CDRL*, 37, 1 (2002).
- [39]D. Wen-Sheng, J. Ki-Won, R. Hyun-Seog, L. Zhong-Wen, P. Sang-Eon, *Catal Lett.*, 78, 1 (2002).
- [40]S. Freni, G. Calogero, S. Cavallaro, *J Power Sources*, 87, 28 (2000).
- [41]J. Dias, J.M. Assaf, *J. Power Sources*, 137, 264 (2004).
- [42]S.Q. Chen, Y. Liu, *Int. J. Hydrogen Energy*, 34, 4735 (2009).
- [43]J. Bessières, A. Bessières, J.J. Heizmann, *Int. J. Hydrogen Energy*, 5, 585 (1980).
- [44]J.A. Peña, E. Lorente, E. Romero, J. Herguido, *Catal. Today*, 116, 3, 439 (2006).
- [45]A. Bonalde, A. Henriquez, M. Manrique, *I.S.I.J. International*, 45, 1255 (2005).
- [46]D. Ghosh, A. Ghosh, *I.S.I.J Transactions* 26, 186 (1986).
- [47]R. Alizadeh, E. Jamshidi, H. Ale-Ebrahim, *Chem. Eng. Technol.*, 30, 1123 (2007).
- [48]H. Ale Ebrahim, E. Jamshidi, *Trans. Inst. Chem. Eng. A*, 79, 62 (2001).
- [49]G.F. Froment, K.B. Bischoff, *Chemical Reaction Analysis and Design*, 2nd Edition John Wiley & Sons, New York. (1990).